International Journal of Materials Lifetime, 2015, Vol. 1, No. 1, 29-39
Available online at http://pubs.sciepub.com/ijml/1/1/5

DOI:10.12691/ijml-1-1-5

A Comparison of Different Porous Structures on the Performance of A Magnetic Fluid Based Double Porous Layered Rough Slider Bearing

Jimit R. Patel*, G. M. Deheri

Department of Mathematics, Sardar Patel University, Vallabh Vidyanagar, Anand-388 120, Gujarat, India
*Corresponding author: patel.jimitphdmarch2013@gmail.com

Received February 26, 2015; Revised April 02, 2015; Accepted April 07, 2015

Abstract An attempt has been made to present an analytical solution for the performance characteristics of a magnetic fluid based double layered porous rough slider bearing. The Kozeny-Carman's model and Irmay's formulation are adopted for porous structures. The stochastic modeling of Christenson and Tonder is employed to evaluate the effect of transverse roughness of the bearing surfaces, in order to develop the associated Reynolds type equation. The expressions for pressure, load and friction are obtained. The graphical representations suggest that the Kozeny-Carman model scores over the Irmay's model for an overall improved performance. It is noticed that the increased load carrying capacity owing to double layered gets enhanced due to the magnetic fluid lubricant and this goes a long way in reducing the adverse effect of roughness in the case of Kozeny-Carman model.

Keywords: *slider bearing, magnetic fluid, porous structure, roughness*

Cite This Article: Jimit R. Patel, and G. M. Deheri, "A Comparison of Different Porous Structures on the Performance of A Magnetic Fluid Based Double Porous Layered Rough Slider Bearing." *International Journal of Materials Lifetime*, vol. 1, no. 1 (2015): 29-39. doi: 10.12691/ijml-1-1-5.

1. Introduction

Among the hydrodynamic bearings, slider bearing is the simplest and frequently encountered because the expression of film thickness is simple and boundary conditions to be required zero at the bearing ends are not that complicated. The fundamental aspect in a hydrodynamic slider bearing is the formation of a conversing wedge of the lubricant. The hydrodynamic slider may be constructed to provide this converging wedge in a number of ways. [1] analyzed the effect of hydrodynamic lubrication of a plane porous slider bearing. It was manifest that the effect of porosity decreased the load carrying capacity and friction. [2] investigated the combined effect of permeability and couple stresses on the performance characteristics of a secant shaped porous slider bearing lubricated with Stokes couple stress fluid. [3] examined a series solution of the long porous slider bearing using the homotopy perturbation method.

Both experimental and analytical researches indicate that lubricant film thickness, surface roughness, material hardness and run-in process have significant effects on lubricated rolling slider bearings. In past, many investigations such as [4-8] accounting for surface roughness effect, have been proposed in order to seek a more realistic representation of bearing surfaces. [9] investigated the stochastic finite element method analysis of finite hydrodynamic bearings with rough surfaces. [10] discussed some mathematical formulae for roughness parameters. [11] analyzed the thermal and roughness effects on different characteristics of an infinite tilted pad slider bearing. It was observed that for a non- parallel slider bearing, the load carrying capacity due to the combined effect was less than the load carrying capacity due to the roughness effect for both models (transverse and longitudinal).

During the last few years a noticeable amount of progress has been made in the research for double layered porous bearings. Many investigations of double layered porous bearings were conducted. [12] presented an analytical solution for the performance characteristics of a double layered porous slider bearing. [13] studied the performance of a double layered porous journal bearing. [14] theoretically analyzed the performance of a double porous layered axially undefined journal bearing lubricated with ferrofluid, considering combined effect of anisotropic permeability of the double layered porous facing. All these studies concluded that the effect of the double layer was to increase the load carrying capacity and the frictional drag but to decrease the coefficient of friction.

Lubrication occurs in engines and machines to reduce friction between the moving plates. Various kinds of fluids are used as lubricants. During the last decade, the use of magnetic fluid has received considerable attention. [15] investigated the effect of ferrofluid lubrication in porous inclined slider bearing. [16] analyzed the performance of a bearing with its slider in exponential form and stator with a porous facing of uniform thickness using a ferrofluid lubricant, considering slip velocity. [17]

considered the theoretical model of a magnetic fluid based porous slider bearing to study the slip velocity effect on the load carrying capacity of the bearing system. [18] discussed dynamic characteristics for magneto hydrodynamic wide slider bearing with an exponential film profile. [19] analyzed the study of a porous rough secant shaped slider bearing under the presence of a magnetic fluid lubricant. [20] investigated the performance of a hydrodynamic short porous journal bearing under the presence of a magnetic fluid lubricant. All these above studies established that the magnetization affected the bearing system positively while the bearing suffered owing to transverse roughness. [21] discussed the comparison of various porous structures on the performance of a magnetic fluid based transversely rough short bearing. Recently, [22] analyzed the combined effect of slip velocity and roughness on the magnetic fluid based infinitely long bearings. It was manifest that keeping the slip coefficient at minimum; the magnetization could compensate the adverse effect of the standard deviation. This study offered an additional degree of freedom through the form of the magnitude of the magnetic field for designing the bearing system.

The aim has been to see which porous structure is more favorable to bearing design even if the bearing has run for a large period. The importance of this study lies in its application aspects especially, to control the diffusion mechanism for the drug-eluting stent and other related applications in tissue engineering.

Here, it has been proposed to deal with the comparison of two different porous structures on the performance of a magnetic fluid based double porous layered rough slider bearing.

2. Analysis

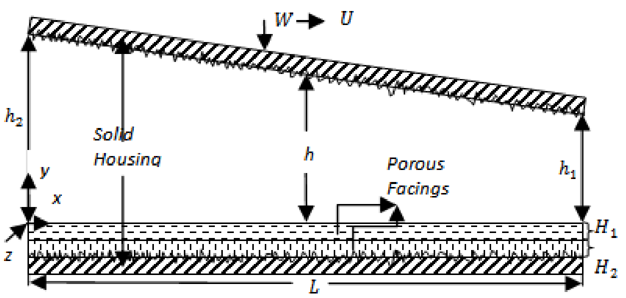

Figure 1A. Configuration of the bearing system

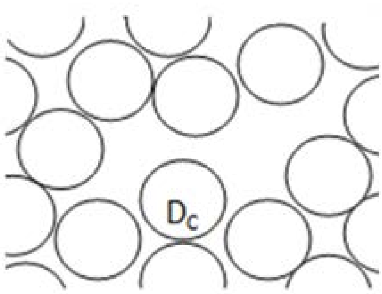

Figure 1B. Kozeny-Carman's model of porous sheets

The geometry and physical configuration of the problem is shown in the Figure 1A. All the assumptions of conventional lubrication theory are retained. For the details one can have a glance at [12]. The porous regions are assumed to be homogeneous and isotropic and the lubricant is incompressible and the flow is laminar. The pressure in porous region satisfies the usual Laplace equation.

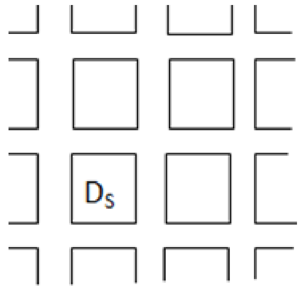

Figure 1C. Irmay's model of porous sheets

It is assumed that the bearing surfaces are transversely rough. According to the stochastic model of [4,5,6], the thickness $h(x)$ of the lubricant film is taken as

$$h(x) = \bar{h}(x) + h_s$$

where $\bar{h}(x)$ is the mean film thickness and h_s is the deviation from the mean film thickness characterizing the random roughness of the bearing surfaces. h_s is governed by the probability density function

$$f(h_s) = \begin{cases} \dfrac{35}{32c^*}\left(1 - \dfrac{h_s^2}{c^{*2}}\right)^3, & -c^* \le h_s \le c^* \\ 0, & elsewhere \end{cases}.$$

wherein c^* is the maximum deviation from the mean film thickness. The mean α, the standard deviation σ and the parameter ε; which is the measure of symmetry of the random variable h_s are defined and discussed in [4,5,6].

Introduction of these assumptions lead to a modified Reynolds equation for the film region, similar to that obtained by ([12])

$$\frac{\partial}{\partial x}\left[\left(h^3 + 12\phi_1 H_1 + 12\phi_2 H_2\right)\frac{\partial p}{\partial x}\right] + \frac{\partial}{\partial z}\left[\left(h^3 + 12\phi_1 H_1 + 12\phi_2 H_2\right)\frac{\partial p}{\partial z}\right] = 6\mu U\frac{dh}{dx} + 12\mu V_h \quad (1)$$

Neglecting the side leakage effect and since there is no normal velocity, equation (1) reduces to

$$\frac{d}{dx}\left[\left(h^3 + 12\phi_1 H_1 + 12\phi_2 H_2\right)\frac{dp}{dx}\right] = 6\mu U\frac{dh}{dx} \quad (2)$$

The magnetic field is taken to be oblique to the stator. [23] investigated the effect of various forms of magnitude of the magnetic field. The magnitude of the magnetic field is taken as

$$M^2 = kx\left(1 - \frac{x}{L}\right)$$

where k is a suitably chosen constant from dimensionless point of view so as to produce a magnetic field of strength over 10^{-23} [24].

Under the usual assumptions of hydro magnetic lubrication ([23,25,26]) developing equation (2) by incorporating the effect of magnetization, the Reynolds equation governing the pressure distribution is obtained as

$$\frac{d}{dx}\left[\begin{array}{c}\left(g(h)+12\phi_1 H_1+12\phi_2 H_2\right)\\ \frac{d}{dx}\left(p-\frac{\mu_0\bar{\mu}M^2}{2}\right)\end{array}\right]=6\mu U\frac{dh}{dx} \tag{3}$$

Where

$$g(h)=h^3+3h^2\alpha+3\left(\sigma^2+\alpha^2\right)h+3\sigma^2\alpha+\alpha^3+\varepsilon$$

while μ_0 is the magnetic susceptibility, $\bar{\mu}$ is the free space permeability, μ is the lubricant viscosity, ϕ_1 is permeability of inner layer, ϕ_2 is permeability of outer layer, H_1 is wall thickness of the inner layer, H_2 is wall thickness of the outer layer, U is tangential velocity of the slider.

The relevant boundary conditions are,

$$p(0)=p(L)=0 \tag{4}$$

The following non dimensional quantities are introduced,

$$\bar{h}=\frac{h}{h_1}=\bar{h}_2-\left(\bar{h}_2-1\right)X,P=\frac{h_1^2}{\mu UL}p,\bar{h}_2=\frac{h_2}{h_1},$$

$$\mu^*=\frac{k\mu_0\bar{\mu}h_1^2}{U\mu},X=\frac{x}{L},\bar{\sigma}=\frac{\sigma}{h_1},\bar{\alpha}=\frac{\alpha}{h_1},\bar{\varepsilon}=\frac{\varepsilon}{h_1^3},$$

$$\bar{\phi}_1=\frac{D_c^2 H_1}{h_1^3},\bar{\phi}_2=\frac{D_s^2 H_2}{h_1^3}$$

Below are discussed the two models regarding the porous regions.

2.1.

A porous material is filled with globular particles (mean particle size D_c) which is given in Figure 1B. The Kozeny-Carman equation is a well-known relation used in the field of fluid dynamics to calculate the pressure drop of a fluid flowing through a packed bed of solids. This equation remains valid only for laminar flow. The Kozeny-Carman equation mimics some experimental trends and hence serves as a quality control tool for physical and digital experimental results. The Kozeny-Carman equation is very often presented as permeability versus porosity, pore size and turtuosity. [27,28,29] suggests that the Kozeny-Carman formula leads to the relation

$$\phi_1=\frac{D_c^2 e^3}{180(1-e)^2}$$

where e is the porosity.

2.2.

In Figure 1C, the model consists of three sets of mutually orthogonal fissures (a mean solid size D_s) and assuming no loss of hydraulic gradient at the junctions, [30,31] derived the permeability

$$\phi_2=\frac{D_s^2\left(1-m^{\frac{1}{3}}\right)^3\left(1+m^{\frac{1}{3}}\right)}{12m}$$

where $m=(1-e)$ and e is the porosity ([32]).

Therefore, the non dimensional two layered permeability for both the cases are defined as

$$H(e)=\begin{cases}2\left(\frac{e^3}{180(1-e)^2}\bar{\phi}_1\right), & \\ \text{for Kozeny}-\text{Carman's Model} & \\ 2\left(\frac{\left(1-m^{\frac{1}{3}}\right)^3\left(1+m^{\frac{1}{3}}\right)}{12m}\bar{\phi}_2\right), & \\ \text{for Irmay's Model} & \end{cases}$$

Using boundary conditions (2) and non dimensional quantities, the dimensionless form of the pressure distribution is found to be

$$P=\frac{\mu^*}{2}X(1-X)+\frac{6}{\left(1-\bar{h}_2\right)}\left[\begin{array}{l}D\ln\left(\bar{h}-J_1\right)+E\ln\left(\bar{h}^2-J_2\bar{h}+J_3\right)\\ +F\tan^{-1}\left(\frac{2\bar{h}-J_2}{\sqrt{4J_3-J_2^2}}\right)+c_2'\left(1-\bar{h}_2\right)\end{array}\right] \tag{5}$$

where

$$D=A+c_1'A_1,E=\frac{1}{2}\left(B+c_1'B_1\right),L_1=\ln\left(\bar{h}_2-J_1\right),$$

$$F=\frac{2\left(C+c_1'C_1\right)+\left(B+c_1'B_1\right)J_2}{\sqrt{4J_3-J_2^2}},L_2=\ln(1-J_1),$$

$$L_3=\ln\left(\bar{h}_2{}^2-J_2\bar{h}_2+J_3\right),L_4=\ln(1-J_2+J_3)$$

$$T_1=\frac{1}{\sqrt{4J_3-J_2^2}}\tan^{-1}\left(\frac{2\bar{h}_2-J_2}{\sqrt{4J_3-J_2^2}}\right)$$

$$T_2=\frac{1}{\sqrt{4J_3-J_2^2}}\tan^{-1}\left(\frac{2-J_2}{\sqrt{4J_3-J_2^2}}\right)$$

$$c_1'=-\frac{\left(\begin{array}{c}A(L_1-L_2)+\left(B/2\right)(L_3-L_4)\\ +(2C+BJ_2)(T_1-T_2)\end{array}\right)}{\left(\begin{array}{c}A_1(L_1-L_2)+\left(B_1/2\right)(L_3-L_4)\\ +(2C_1+B_1J_2)(T_1-T_2)\end{array}\right)}$$

$$c_2' = \frac{1}{\left(1-\bar{h}_2\right)}\left[\begin{array}{c} DL_1 + EL_3 \\ +\left\{\begin{array}{c} 2\left(C + c_1' C_1\right) \\ +\left(B + c_1' B_1\right) J_2 \end{array}\right\} T_1 \end{array}\right]$$

$$a = 3\bar{\alpha}, b = 3\left(\bar{\alpha}^2 + \bar{\sigma}^2\right), c = \bar{\alpha}^3 + 3\bar{\sigma}^2\bar{\alpha} + \bar{\varepsilon} + 12H(e)$$

$$J = \sqrt[3]{-2a^3 + 3\sqrt{3}J' + 9ab - 27c}$$

$$J' = \sqrt{4a^3c - a^2b^2 - 18abc + 4b^3 + 27c^2}$$

$$J_1 = \frac{J}{3\sqrt[3]{2}} - \frac{\sqrt[3]{2}\left(3b - a^2\right)}{3J} - \frac{a}{3}, B_1 = -A_1$$

$$J_2 = -2\frac{J}{6\sqrt[3]{2}} + 2\frac{\left(3b - a^2\right)}{(3)(2^{2/3})J} - \frac{2a}{3}, B = -A$$

$$J_3 = \left[4\left(\frac{J}{6\sqrt[3]{2}}\right)^2 + 4\left(\frac{J}{6\sqrt[3]{2}}\right)\left(\frac{\left(3b - a^2\right)}{(3)(2^{2/3})J}\right)\right.$$

$$\left. +4\left(\frac{\left(3b - a^2\right)}{(3)(2^{2/3})J}\right)^2 + 2\left(\frac{J}{6\sqrt[3]{2}}\right)\frac{a}{3} - 2\left(\frac{\left(3b - a^2\right)}{(3)(2^{2/3})J}\right)\frac{a}{3} + \frac{a^2}{9}\right],$$

$$A = \frac{J_1}{J_1^2 - J_1J_2 + J_3}, C = \frac{J_3}{J_1^2 - J_1J_2 + J_3},$$

and

$$A_1 = \frac{1}{J_1^2 - J_1J_2 + J_3}, C_1 = \frac{J_2 - J_1}{J_1^2 - J_1J_2 + J_3}$$

The non dimensional load carrying capacity of the bearing system then, turns out to be

$$\begin{aligned} W &= \frac{h_1^2 w}{\mu UBL^2} \\ &= \frac{\mu^*}{12} + \frac{6}{\left(1-\bar{h}_2\right)^2}\left[DI_1 + EI_2 + FI_3 + c_2'\left(1-\bar{h}_2\right)^2\right] \end{aligned} \tag{6}$$

where

$$I_1 = (1 - J_1)(L_2 - 1) - \left(\bar{h}_2 - J_1\right)(L_1 - 1)$$

$$I_2 = -2\left(1 - \bar{h}_2\right) + \left(4J_3 - J_2^2\right)(T_2 - T_1)$$

$$+\left(\frac{2 - J_2}{2}\right)L_4 - \left(\frac{2\bar{h}_2 - J_2}{2}\right)L_3$$

and

$$I_3 = \sqrt{4J_3 - J_2^2}\left\{\begin{array}{c} \left(\frac{2 - J_2}{2}\right)T_2 \\ -\left(\frac{2\bar{h}_2 - J_2}{2}\right)T_1 \\ +\frac{1}{4}\left(L_3 - L_4\right) \end{array}\right\}$$

Therefore, the dimensionless frictional drag exerted by the moving slider takes the form

$$\begin{aligned} F &= \frac{fh_1}{\mu UBL} = \int_0^1\left(\frac{\bar{h}}{2}\frac{\partial P}{\partial X} + \frac{1}{\bar{h}}\right)dX \\ &= \frac{1}{\left(\bar{h}_2 - 1\right)}\left\{\frac{\left(\bar{h}_2 - 1\right)^2}{2}W + \ln\left(\bar{h}_2\right)\right\} \end{aligned} \tag{7}$$

3. Results and Discussion

It is noticed that the non- dimensional pressure increases by

$$\frac{\mu^*}{2}X(1 - X)$$

while the increase in the dimensionless load carrying capacity is

$$\frac{\mu^*}{12}$$

as compared to the case of conventional fluid based bearing systems. The load carrying capacity in dimensionless form gets enhanced by at least 1% as compared to [12] for a smooth bearing system. Probably, this is due to the fact that the magnetization induces an increase in the viscosity of the lubricant. As the expression involved in (6) is linear with respect to the magnetization, an increase in magnetization parameter would eventually lead to increased load carrying capacity.

As can be seen, Figure 2- Figure 15 concern with the comparison of load carrying capacity when porosity of both layers is either governed by Kozeny-Carman's model or Irmay's model for the permeability structure. Besides, the comparison of friction is provided in Figure 16- Figure 29 for the above mentioned both porous structures.

The variation of load carrying capacity with respect to $\bar{h}_2$ is exhibited in Figure 2- Figure 6. As can be seen from Figures 2-6 the load carrying capacity is more reduced in the case of Irmay's model. Probably, this may be due to the fact that the motion of the lubricant gets unevenly opposed and the pressure drop is more [30]. However, the reduction remains almost marginal.

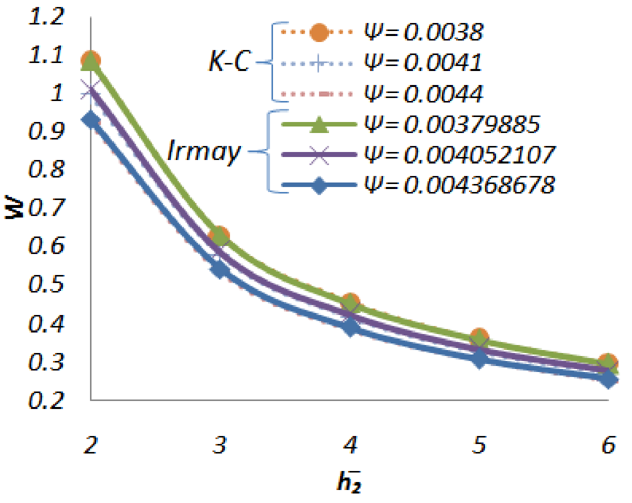

Figure 2. Variation of load carrying capacity with respect to $\bar{h}_2$ and ψ .

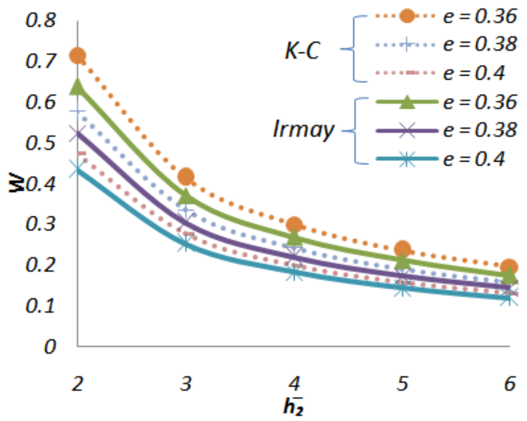

Figure 3. Variation of load carrying capacity with respect to $\bar{h}_2$ and e

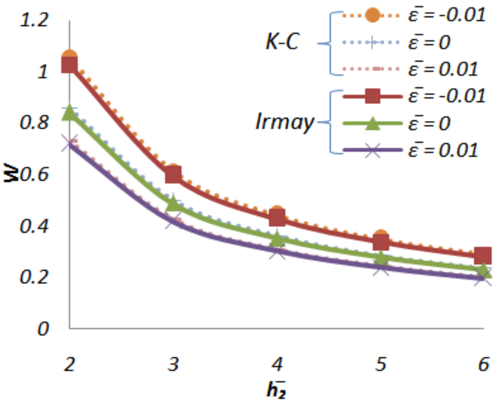

Figure 4. Variation of load carrying capacity with respect to $\bar{h}_2$ and $\bar{\varepsilon}$.

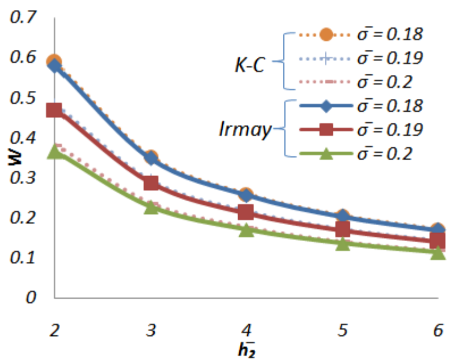

Figure 5. Variation of load carrying capacity with respect to $\bar{h}_2$ and $\bar{\sigma}$.

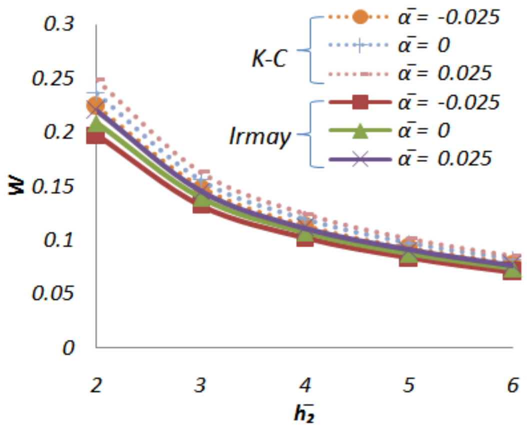

Figure 6. Variation of load carrying capacity with respect to $\bar{h}_2$ and $\bar{\alpha}$.

The bearing system gets adversely affected owing to transverse roughness as the motion of the lubricant gets obstructed by roughness.

Figure 7- Figure 9 present the variation of load carrying capacity with respect to the combined porous structures parameter. It is observed that the negatively skewed roughness and variance (-ve) cause increased load carrying capacity and this load carrying capacity is registered to be more in the case of Kozeny-Carman model. Further, the positive skewness, variance (+ve) and standard deviation turn in diminished load carrying capacity. This is because the obstruction rendered by standard deviation is relatively more in the case of Irmay's model. Therefore, it is not difficult to see that here also the Kozeny-Carman model remains superior to Irmay's model, so far as the adverse effect of roughness is concerned.

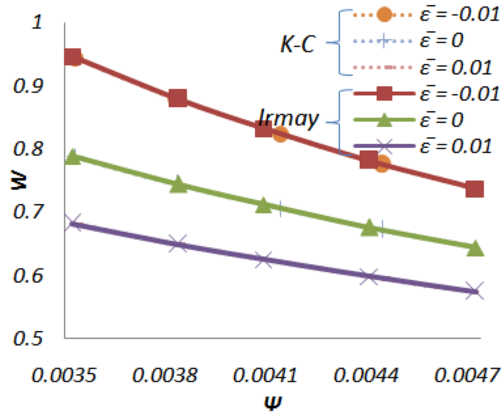

Figure 7. Variation of load carrying capacity with respect to ψ and $\bar{\varepsilon}$.

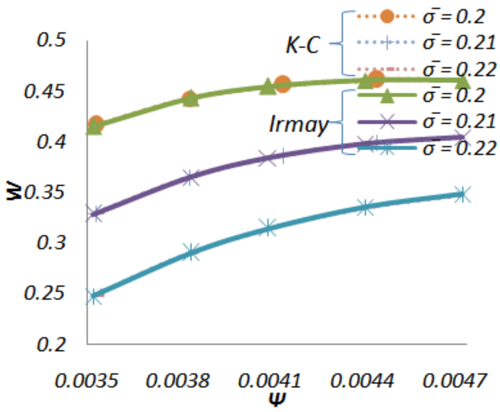

Figure 8. Variation of load carrying capacity with respect to ψ and $\bar{\sigma}$.

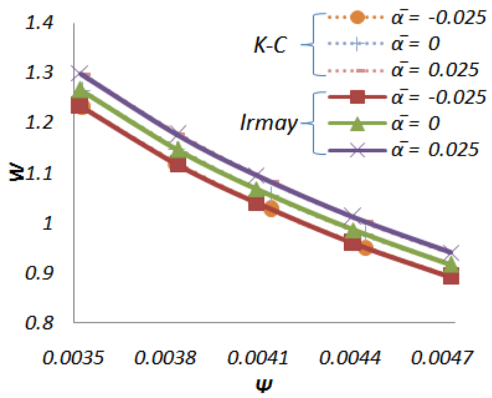

Figure 9. Variation of load carrying capacity with respect to ψ and $\bar{\alpha}$.

The effect of porosity given in Figure 10- Figure 12 indicates that the porosity follows the path of porous structure parameter in reducing the load carrying capacity. The adverse effect of both the parameters associated with porosity is found to be comparatively more in the case of Irmay's model. It is well known from [30] that the pressure drop is more in the case of Irmay's model and hence the related decreased load.

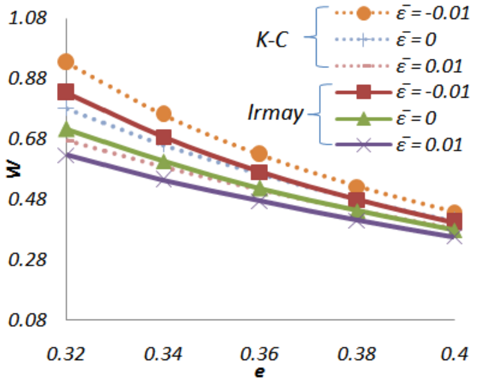

Figure 10. Variation of load carrying capacity with respect to e and $\bar{\varepsilon}$.

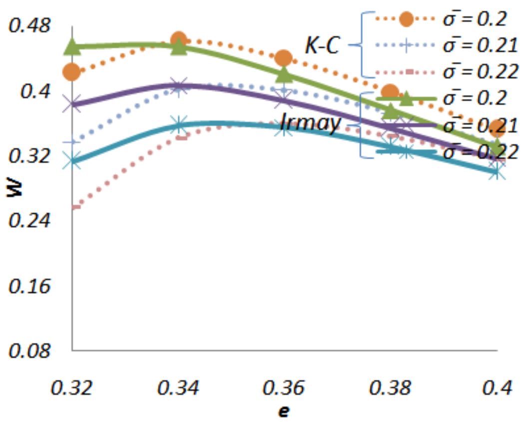

Figure 11. Variation of load carrying capacity with respect to e and $\bar{\sigma}$.

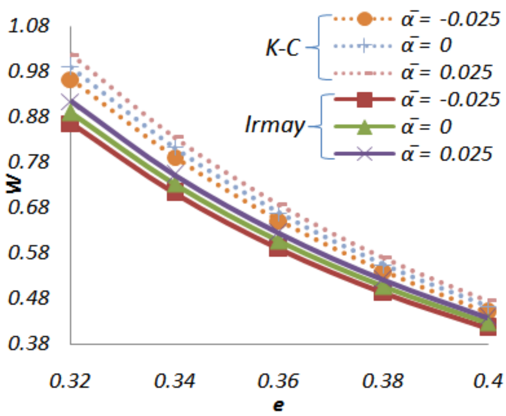

Figure 12. Variation of load carrying capacity with respect to e and $\bar{\alpha}$.

The effect of skewness presented in Figure 13- Figure 14 suggest that positively skewed roughness decreases the load carrying capacity while the load carrying capacity increases due to negatively skewed roughness. Similar is the trends of variance so far as the load carrying capacity is concerned (Figure 15). This may be due to the fact that positive skewness opposes (although in a small quantity) the flow of the lubricant which is further aided by variance (+ve).

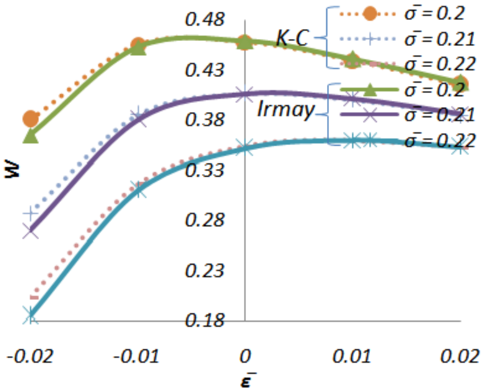

Figure 13. Variation of load carrying capacity with respect to $\bar{\varepsilon}$ and $\bar{\sigma}$.

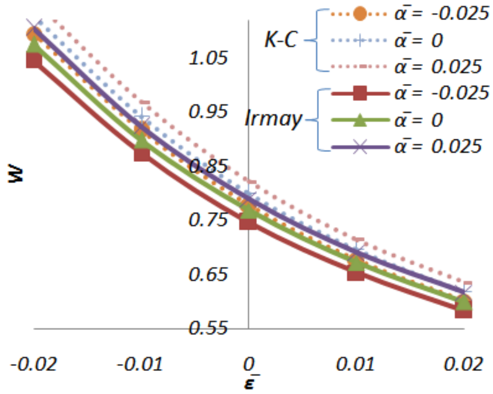

Figure 14. Variation of load carrying capacity with respect to $\bar{\varepsilon}$ and $\bar{\alpha}$.

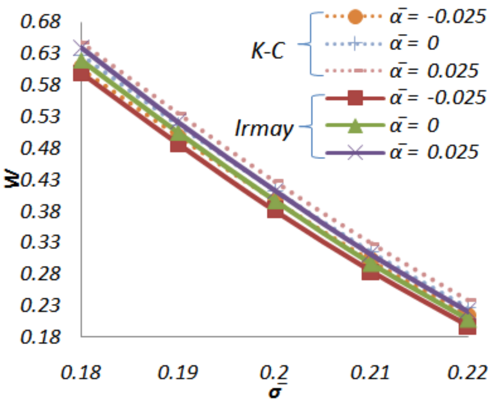

Figure 15. Variation of load carrying capacity with respect to $\bar{\sigma}$ and $\bar{\alpha}$.

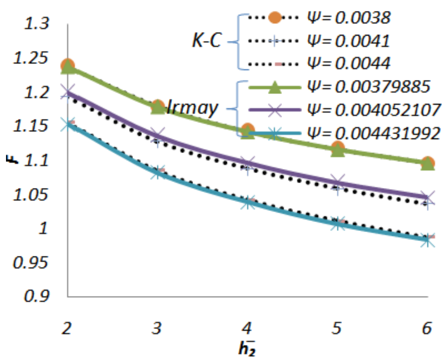

Figure 16. Variation of Friction with respect to $\bar{h}_2$ and ψ .

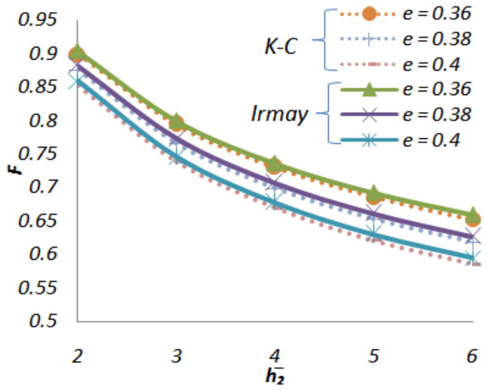

Figure 17. Variation of Friction with respect to $\bar{h}_2$ and e.

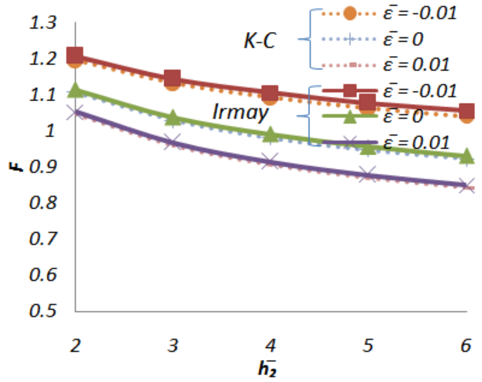

Figure 18. Variation of Friction with respect to $\bar{h}_2$ and $\bar{\varepsilon}$.

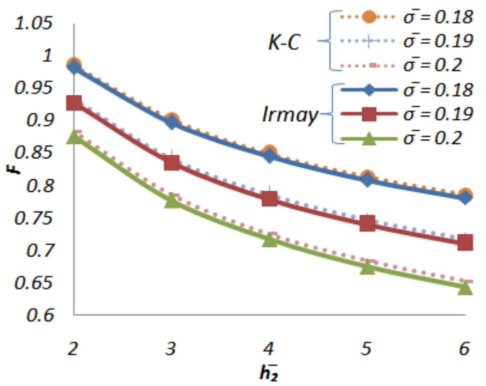

Figure 19. Variation of Friction with respect to $\bar{h}_2$ and $\bar{\sigma}$.

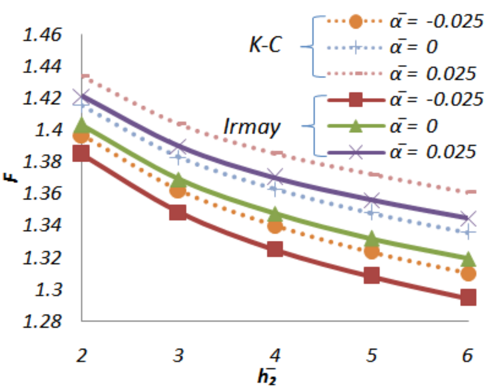

Figure 20. Variation of Friction with respect to $\bar{h}_2$ and $\bar{\alpha}$.

The variation of friction presented in Figure 16- Figure 20 makes it clear that $\bar{h}_2$ reduces the friction in a good way. Further, the reduction of friction is found to be more (although in a small quantity) in the case of Kozeny-Carman model.

Likewise, the porous structure brings down the friction as can be seen from Figure 21- Figure 23. From Figure 22 it is clear that porous structure introduces a negligible increase in the friction as well. A close scrutiny of these figures reveals that the friction reduction remains quite significant even if the bearing has run for a longer period even in the case of Kozeny-Carman model.

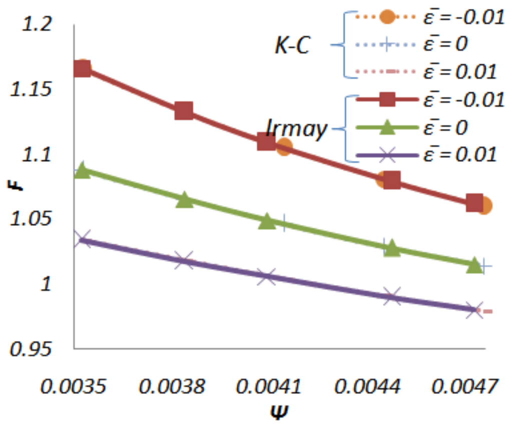

Figure 21. Variation of Friction with respect to ψ and $\bar{\varepsilon}$.

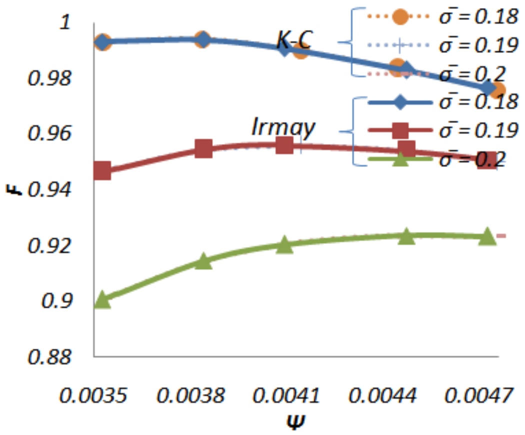

Figure 22. Variation of Friction with respect to ψ and $\bar{\sigma}$.

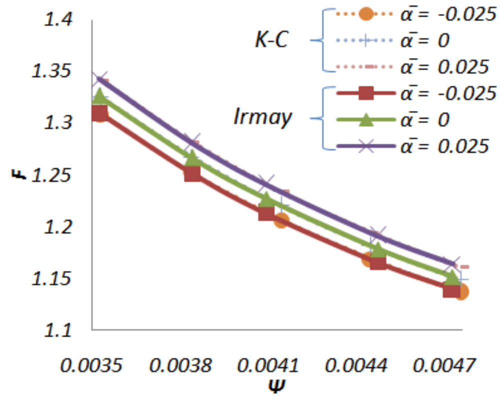

Figure 23. Variation of Friction with respect to ψ and $\bar{\alpha}$.

The porosity parameter reduces the friction in a rapid way which is manifest in Figure 24- Figure 26. For smaller values of standard deviation and porosity parameter the friction increases and it decreases significantly after words (Figure 25).

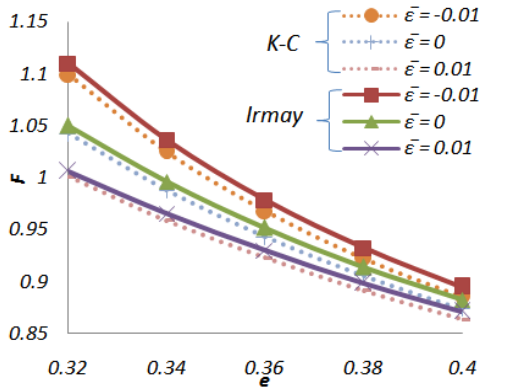

Figure 24. Variation of Friction with respect to e and $\bar{\varepsilon}$.

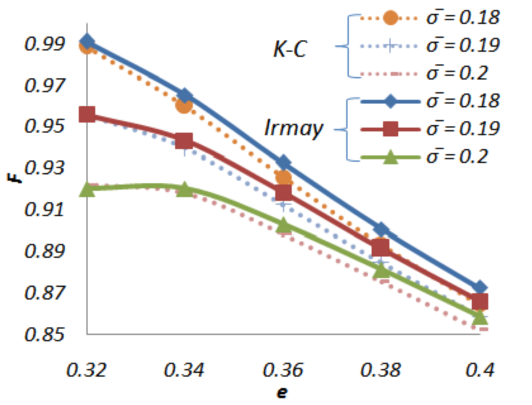

Figure 25. Variation of Friction with respect to e and $\bar{\sigma}$.

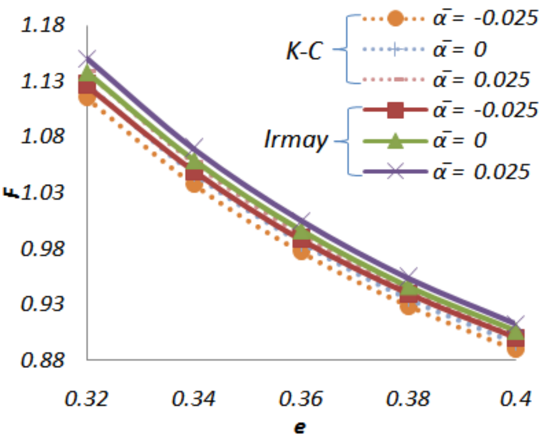

Figure 26. Variation of Friction with respect to e and $\bar{\alpha}$.

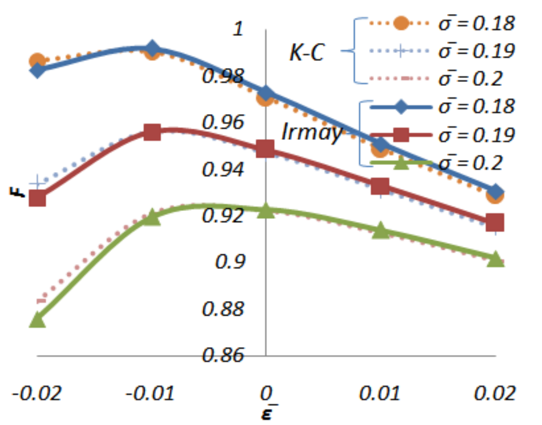

Figure 27. Variation of Friction with respect to $\bar{\varepsilon}$ and $\bar{\sigma}$.

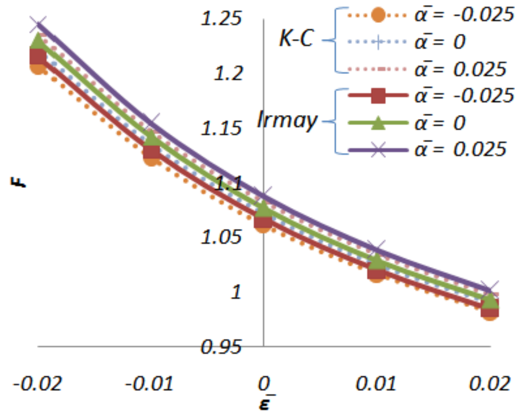

Figure 28. Variation of Friction with respect to $\bar{\varepsilon}$ and $\bar{\alpha}$.

The effect of positive skewness is to decrease the friction which gets further decreased due to positive variance which can be seen from Figure 27- Figure 28.

Figure 29 presents the variation of friction with respect to the standard deviation. Of course there is marginal increase in friction due to magnetization.

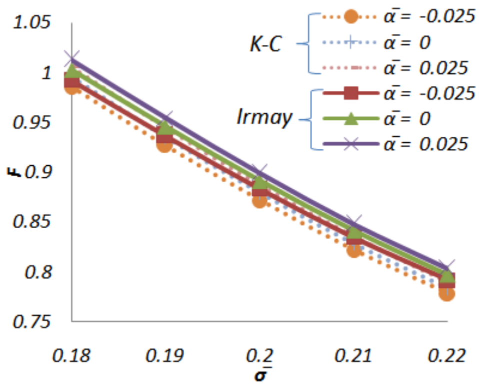

Figure 29. Variation of Friction with respect to $\bar{\sigma}$ and $\bar{\alpha}$.

It is seen that the effect of transverse roughness on the variation of load carrying capacity with respect to the porous structures is almost negligible for this type of bearing system. Thus, there is no variation of friction with respect to the porous structure for different values of roughness parameters.

For smaller values of the porosity, Kozeny-Carman model registers more increase in load carrying capacity as compared to Irmay's formulation so far as the effect of standard deviation is concerned. Also, the decrease in friction is more in Kozeny-Carman model in comparison with the Irmay's model.

It is interesting to note that the increase in load carrying capacity is more in the case of Kozeny-Carman model for smaller values of skewness (up to -0.01) so far as the effect of standard deviation is concerned. In fact, the load carrying capacity after words decreases for both the models. The decrease in friction is found to be more in the case of Irmay's model.

Some of the graphs presented here, suggest that the magnetization may provide a little help in reducing the adverse effect of roughness and $\bar{h}_2$ even in the case of negatively skewed roughness for Irmay's model but the situation eases in Kozeny-Carman's model.

One has to reckon that the role of $\bar{h}_2$ is quite significant for improving the performance of the bearing system.

The increased load carrying capacity due to magnetization gets further increased by the existence of double layer, this effect being more in case Kozeny-Carman model is taken into consideration.

The effect of double layer is observed to decrease the friction force rapidly when Kozeny-Carman model is considered.

The least rise in the load carrying capacity due to negatively skewed roughness in the case of Kozeny-Carman model is by 2.3% approximately and this is approximately 1.4% in the case of Irmay's model. Likewise, the load carrying capacity rises by close to 3% due to variance(-ve) in the Kozeny-Carman model while this increase in the load is by 2.3% in the case of Irmay's model.

4. Validation

The conclusions are validated by giving a comparison of the load and friction of this investigation with some results from already published works. It is noticed that the load carrying capacity goes up at least by 1%. The results presented here jell well with those of the published article. However, here the load is substantially increased owing to the magnetization, in spite of the adverse effect of roughness. However, as can be observed there is a marginal decrease in the friction here. (I- the load carrying capacity/Friction of [12], II- the load carrying capacity/Friction of this manuscript for Kozeny-Carman model, III- the load carrying capacity/Friction of this manuscript for Irmay's model).

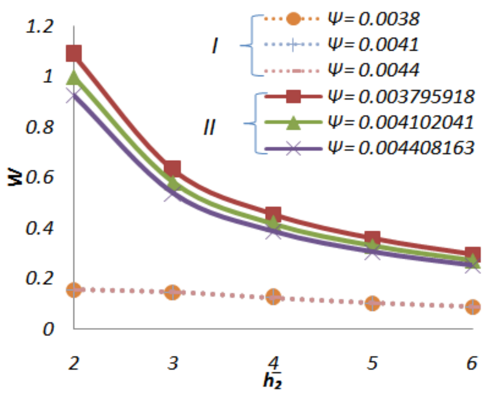

Figure 30. Variation of load carrying capacity with respect to $\bar{h}_2$ and ψ .

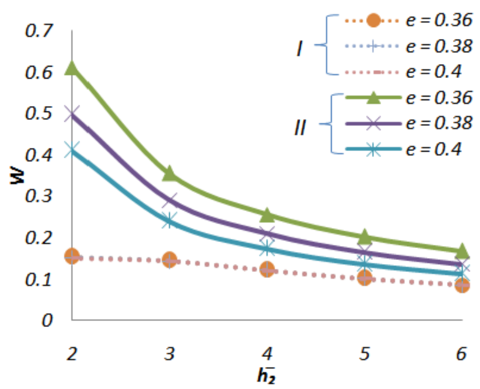

Figure 31. Variation of load carrying capacity with respect to $\bar{h}_2$ and e .

A close glance at the Figure 30- Figure 37 tends to suggest that the rate of decrease in the load carrying capacity gets decreased by more than 3% in the case of Kozeny-Carman model while the rate of friction decrease is 3.68% in comparison with the study of [12].

Further, the rate of decrease in the load carrying capacity decreases by just 1.5% in the case of Irmay's model and the rate of reduction in the friction gets reduced by 1.8%.

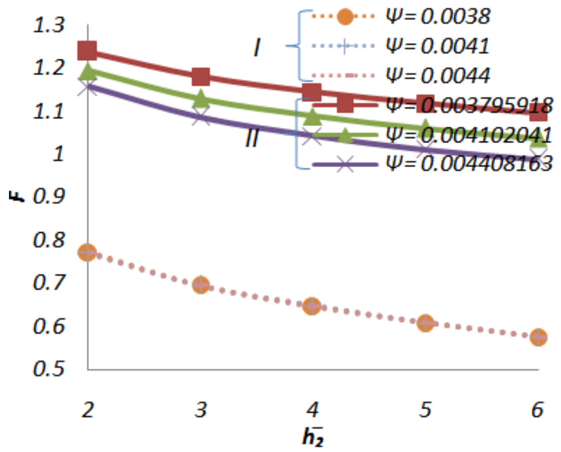

Figure 32. Variation of Friction with respect to $\bar{h}_2$ and ψ ..

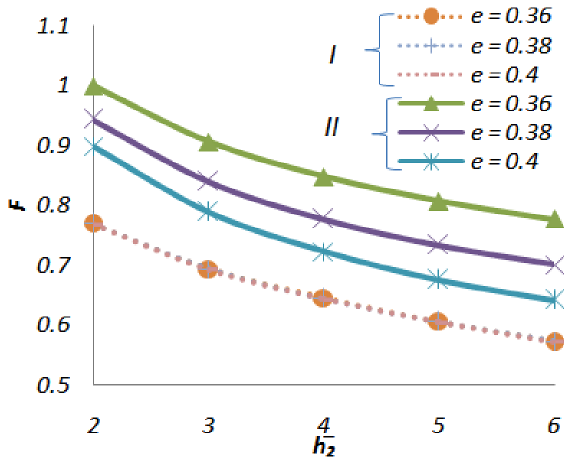

Figure 33. Variation of friction with respect to $\bar{h}_2$ and e .

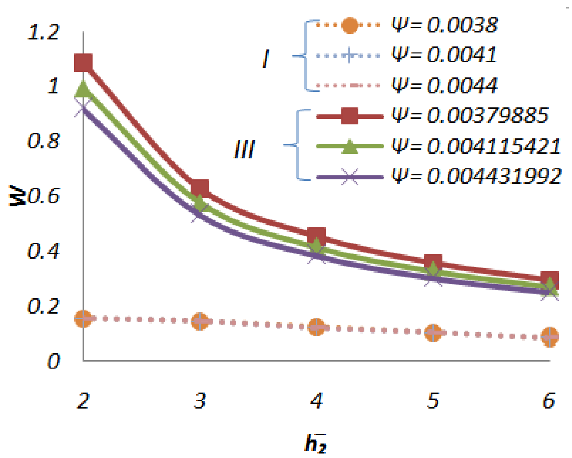

Figure 34. Variation of load carrying capacity with respect to $\bar{h}_2$ and ψ .

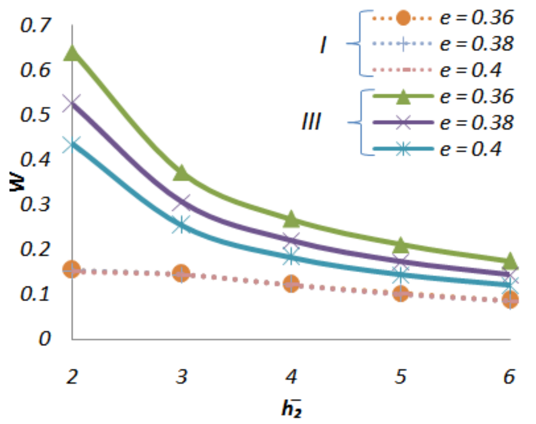

Figure 35. Variation of load carrying capacity with respect to $\bar{h}_2$ and e .

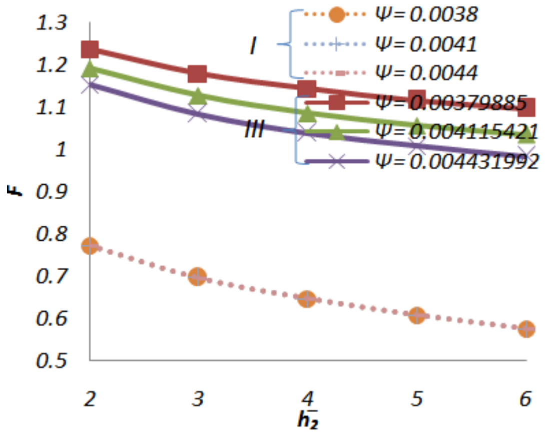

Figure 36. Variation of Friction with respect to $\bar{h}_2$ and ψ .

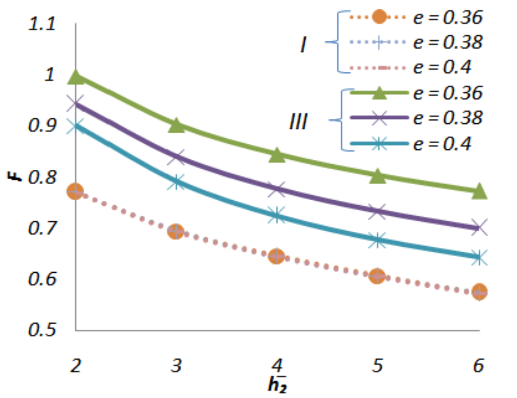

Figure 37. Variation of Friction with respect to $\bar{h}_2$ and e .

5. Conclusion

An important observation is that this type of bearing system supports a good amount of load even in the absence of flow unlike the case of a conventional lubricant based bearing system and this load supporting capacity is found to be more in the case of Kozeny-Carman model. It is appealing to note that the porous structure parameter for both the models causes an increase in the load carrying capacity with respect to the standard deviation. This can be channelized while designing the bearing system. This investigation reveals that the Kozeny-Carman model registers a superior performance as compared to Irmay's model even if double layered is in place. The Kozeny-Carman model may be preferred from bearing's life period point of view. This is all the more necessary when the bearing has put in a long run.

Acknowledgement

One of the authors, Mr. Jimit R. Patel acknowledges the financial assistance of the UGC-BSR Research Scholarship provided by UGC, India. The authors acknowledge with thanks the fruitful comments and suggestions of reviewers/Editors, leading to an improvement in the presentation of this paper.

References

[1] Prakash, J. and Vij, S.K., "Hydrodynamic Lubrication of a porous Slider," *Journal of Mechanical engineering science*, 15 (3), 232-234, 1973.

[2] Bujurke, N.M., Naduvinamani N.B. and Benchalli, S.S., "Secant shaped porous slider bearing lubricated with couple stress fluids," *Industrial Lubrication and Tribology*, 57 (4), 155-160, 2005.

[3] Khan, Y., Faraz, N, Yildirim, A., Wu, Q., "A series solution of the long porous slider," *Tribology Transactions*, 54, 187-191, 2011.

[4] Christensen, H. and Tonder, K.C., "Tribology of rough surfaces: stochastic models of hydrodynamic lubrication," *SINTEF*, Report No.10/69-18,1969a.

[5] Christensen, H. and Tonder, K.C., "Tribology of rough surfaces: parametric study and comparison of lubrication models," *SINTEF*, Report No.22/69-18, 1969b.

[6] Christensen, H. and Tonder, K.C., "The hydrodynamic lubrication of rough bearing surfaces of finite width," *ASME-ASLE Lubrication Conference, Cincinnati, OH,* Paper no. 70-lub-7, 12-15, 1970.

[7] Prajapati, B. L., "Behaviour of squeeze film between rotating porous circular plates: surface roughness and elastic deformation effects," *Pure and Applied Mathematical Science*, 33 (1-2), 27-36, 1991.

[8] Gupta, J.L. and Deheri, G.M., "Effect of Roughness on the Behavior of Squeeze Film in a Spherical Bearing,' *Tribology Transactions*, 39, 99-102, 1996.

[9] Turaga, Ram, Sekhar, A.S. and Majumdar, B.C., "Stochastic FEM analysis of finite hydrodynamic bearings with rough surfaces," *Tribology Transactions*, 40 (4), 605-612, 1997.

[10] Gadelmawla, E.S., Koura, M.M., Maksoud, T.M.A., Elewa, I.M. and Sollman, H.H., "Roughness parameters," *Journal of materials processing Technology*, 123 (1), 133-145, 2002.

[11] Sinha, Prawal and Adamu, Getachew, "THD analysis for slider bearing with roughness: special reference to load generation in parallel sliders," *Acta Mech.*, 207, 11-27, 2009.

[12] Srinivasan, U., "The analysis of a double-Layered porous slider bearing," *Wear*, 42, 205-215, 1977.

[13] Verma, P.D.S., "Double layer porous journal bearing," *Mechanics of Materials*, 2 (3), 233-238, 1983.

[14] Shah R.C. and Patel, D.B., "Mathematical analysis of newly designed ferrofluid lubricated double porous layered axially undefined journal bearing with anisotropic permeability, slip velocity and squeeze velocity," *International journal of fluid mechanics research*, 40 (5), 446-454, 2013.

[15] Ram, Paras and Verma, P.D.S., "Ferrofluid lubrication in porous inclined slider bearing", *Indian J. Pure Appl. Math.*, 30 (12), 1273-1281, 1999.

[16] Shah, R.C. and Bhat, M.V., "Lubrication of a porous exponential slider bearing by ferrofluid with slip velocity", *Turkish J. Engg. Env. Sci.*, 27, 183-187, 2003.

[17] Ahmad, N. and Singh J.P., "Analysis of a porous inclined slider bearing lubricated with a magnetic fluid considering slip velocity," *Proceedings of the institution of Mechanical Engineers, Part N: Journal of Nanoengineering and Nanosystems*, 221 (3), 81-85, 2007.

[18] Lin, J.R. and Lu, R.F., "Dynamic characteristics for magneto hydrodynamic wide slider bearing with an exponential film

rofile," *Journal of Marine Science and Technology*, 18, 268-276, 2010.

[19] Shukla, S.D. and Deheri, G.M., "Surface roughness effect on the performance of a magnetic fluid based porous secant shaped slider bearing," *Industrial Engineering letters*, 1 (2), 12-25, 2011.

[20] Patel, N.S., Vakharia, D.P. and Deheri, G.M., "A study on the performance of a magnetic fluid based hydrodynamic short porous journal bearing, *Journal of the Serbian society for computational mechanics*, 6 (2), 28-44, 2012.

[21] Patel, J.R. and Deheri, G.M., "A comparison of porous structures on the performance of a magnetic fluid based rough short bearing," *Tribology in industry*, 35 (3), 177-189, 2013.

[22] Patel, J. R. and Deheri, G., "Slip velocity and roughness effect on magnetic fluid based infinitely long bearings," *Proceedings of international conference on advances in Tribology and Engineering Systems*, Springer India, 97-109, 2014.

[23] Prajapati, B.L., "On Certain Theoretical Studies in Hydrodynamic and Electro-magneto hydrodynamic Lubrication," *Ph. D. Thesis*, S.P. University, Vallabh Vidyanagar, 1995.

[24] Bhat, M.V. and Deheri, G.M., "Porous slider bearing with squeeze film formed by a magnetic fluid," *Pure and Applied Mathematika Sciences*, 39 (1-2), 39-43, 1995.

[25] Bhat, M.V., *Lubrication with a Magnetic fluid*, Team Spirit (India) Pvt. Ltd, 2003.

[26] Deheri, G.M., Andharia, P.I. and Patel, R.M., "Transversely rough slider bearings with squeeze film formed by a magnetic fluid," *Int. J. of Applied Mechanics and Engineering*, 10 (1), 53-76, 2005.

[27] Liu, J., "Analysis of a porous elastic sheet damper with a magnetic fluid," *Journal of Tribology*, 131, 0218011-15, 2009.

[28] Patel, J.R. and Deheri G., "Shliomis model based ferrofluid lubrication of squeeze film in rotating rough curved circular disks with assorted porous structures," *American journal of Industrial Engineering*, 1 (3), 51-61, 2013.

[29] Patel, J.R. and Deheri G., "Effect of various porous structures on the Shliomis model based ferrofluid lubrication of the film squeezed between rotating rough curved circular plates," *Facta Universitatis, Series: Mechanical Engineering*, 12 (3), 305-323, 2014.

[30] Bear, J., Zaslavsky, D. and Irmay, S., *Physical Principles of Water Percolation and Seepage*, Unesco, Paris, France, 1968.

[31] Patel, J.R., Deheri, G., "Shliomis model-based magnetic squeeze film in rotating rough curved circular plates: a comparison of two different porous structures," *Int. J. Computational Materials Science and Surface Engineering*, 6 (1), 29-49, 2014.

[32] Patel, J.R. and Deheri G., "Theoretical study of Shliomis model based magnetic squeeze film in rough curved annular plates with assorted porous structures," *FME Transactions*, 42 (1), 56-66, 2014.